

A Possible Mechanism for Overcoming the Electrostatic Barrier Against Dust Growth in Protoplanetary disks

V.V. Akimkin^{1,2}

¹*Institute of Astronomy, Russian Academy of Sciences, Moscow, Russia*

²*St. Petersburg State University, V.V. Sobolev Astronomical Institute, St. Petersburg, Russia*

Received December 11, 2014. Accepted January 22, 2015.

akimkin@inasan.ru

ABSTRACT

The coagulation of dust particles under the conditions in protoplanetary disks is investigated. The study focuses on the repulsive electrostatic barrier against growth of charged dust grains. Taking into account the photoelectric effect leads to the appearance of a layer at intermediate heights where the dust has a close to zero charge, enabling the dust grains to grow efficiently. An increase in the coagulation rate comes about not only due to the lowering of the Coulomb barrier, but also because of the electrostatic attraction between grains of opposite charge due to the non-zero dispersion of the near-zero charge. Depending on the efficiency of mixing in the disk, the acceleration of the evolution of the dust in this layer could be important, both in the quasi-stationary stage of the disk evolution and during its dispersal.

DOI: 10.1134/S1063772915070021

1 INTRODUCTION

The first attempts to describe the growth of particles due to their coagulation were made by Smoluchowski (Smoluchowski 1916) in 1916. He presented an equation (the so-called Smoluchowski equation) describing the agglomeration of colloidal particles undergoing Brownian motion. The methods of the coagulation theory were adapted to the study of processes in the late, gravity-assisted accumulation of macroscopic pre-planetary bodies by Safronov (Safronov 1969). Subsequently, these methods have also been widely applied to theoretical modeling of the early stages of the evolution of protoplanetary disks (Schmitt, Henning & Mucha 1997; Tanaka, Himeno & Ida 2005; Nomura & Nakagawa 2006; Birnstiel, Dullemond & Brauer 2010; Akimkin et al. 2013).

In spite of successes in theoretical modeling of the evolution of dust in protoplanetary disks (Testi et al. 2014), many important problems remain to be solved. These include so-called growth barriers, which hinder the formation of macroscopic dust particles ($\gtrsim 1$ cm in size). The first of these barriers (arising earliest in the evolution of the disk) is the electrostatic repulsion between dust grains with the same sign of charge (Okuzumi 2009; Matthews, Land & Hyde 2012). Due to the negative charge of the grains in deep layers of the disk, an appreciable suppression of the dust coagulation can arise, even causing this process to fully cease. As was noted in Okuzumi et al. (2011b), overcoming the Coulomb barrier is possible under the conditions of strong turbulence ($\alpha \gtrsim 10^{-2}$), but this can have an adverse effect on the growth of larger grains due to fragmentation during collisions. Overall, possible ways to overcome the electrostatic barrier have been relatively little studied, compared to barriers to dust growth arising at later stages in the evolution of protoplanetary disks.

Although the charge of dust is an important (if not the determining) factor in its dynamics and evolution, the coagulation

of even neutral dust grains can be suppressed by various mechanisms. For example, grains become more compact due to collisions, which increases the probability that they will bounce, rather than coagulate. This leads to a reduction in the growth of the grains and the appearance of a so-called bouncing barrier (Zsom et al. 2010). As the dust grains grow, their relative velocity increases due to their radial drift (Weidenschilling 1977) and turbulence induced motion (Voelk et al. 1980). If the collision velocity exceeds some critical value (~ 10 m/s), the collisions likely lead to fragmentation, rather than agglomeration, of the grains — the so-called fragmentation barrier (Blum & Wurm 2008; Wada et al. 2009; Teiser & Wurm 2009). Radial drift can remove large grains from the disk so quickly that they simply are not able to grow during their motion toward the central star (Brauer, Dullemond & Henning 2008). This imposes strong lower limits on the rate of coagulation of the particles in protoplanetary disks at the final stages of evolution (the radial-drift barrier).

Only collisional charging is usually considered in modeling of the coagulation of charged dust grains (Okuzumi 2009; Okuzumi et al. 2011b; Matthews, Land & Hyde 2012). In this case, under the conditions near the midplane of a protoplanetary disk, nearly all the grains are negatively charged. However, in the atmosphere of the disk, where the photoelectric effect becomes important, the dust grains are instead strongly positively charged (Pedersen & Gómez de Castro 2011). Accordingly, there must exist a region at intermediate heights where the grains have zero charge, or even opposite charges (due to the dispersion of the charge in the ensemble of grains), which can potentially appreciably increase the coagulation rate. In our study, we investigated the possibility and conditions for the growth of charged dust in a layer of grains with near-zero charge for the typical conditions of a protoplanetary disk.

Note that numerous interesting effects in dusty plasmas have

been discovered in experiments under microgravity conditions on-board the Mir space station Fortov et al. (2004), and also subsequently on-board the International Space Station. In particular, an anomalous increase in the rate of coagulation of charged grains (by four to five orders of magnitude) was found, compared to the case of neutral grains (Konopka et al. 2005).

The structure of the paper is as follows. Section 2 describes the method used, and a discrete equation for the coagulation of charged grains with a non-zero charge dispersion is presented. Section 3 presents the results of dust grain coagulation modeling in a protoplanetary disk for neutral dust and two cases of charged dust. Section 4 discusses dynamical aspects of the evolution of grains and the extent to which the adopted assumptions influence the modeling results. The Conclusion summarizes the main conclusions of our study.

2 COAGULATION THEORY APPLIED TO THE GROWTH OF CHARGED GRAINS

2.1 General Form of the Coagulation Equation

The Smoluchowski equation can be written in two forms — integral and discrete. The former considers the continuous distribution of the particle masses, $f(m)$ [$\text{cm}^{-3} \text{g}^{-1}$], where $f(m)dm$ is the number density of particles with masses within dm of m . The distribution $f(m)$ is normalized to the total number density of dust particles $n_d = \int f(m)dm$. The coagulation rate for particles with masses m_1 and m_2 is specified by the coagulation kernel $K(m_1, m_2)$, which is proportional to the collisional cross section, the velocity of the colliding particles, and the sticking probability. In the integral form, the evolution of the distribution function $f(m)$ is given by the equation

$$\begin{aligned} \frac{\partial f(m, t)}{\partial t} = & \frac{1}{2} \int_0^m f(m-m', t) f(m', t) K(m-m', m') dm' - \\ & - f(m, t) \int_0^\infty f(m', t) K(m, m') dm'. \end{aligned} \quad (1)$$

The first term here describes the coagulation of particles with masses $m-m'$ and m' , leading to the formation of a particle with mass m . The second term is negative and corresponds to the disappearance of particles with mass m due to their coagulation with all other particles. An analytical solution to this equation can be found only for the simplest coagulation kernels — constant (Smoluchowski 1916) and linear (Safronov 1969). These kernels are not suitable for the conditions in a protoplanetary disk, but can be used to test algorithms for the solution of the Smoluchowski equation. A numerical approach can be used with more realistic kernels. A solution of this equation for the conditions in a protoplanetary disk is presented, for example, in Dullemond & Dominik (2005).

The discrete form of the coagulation equation describes the variations in the number densities $\{N_k\}_{k=1}^\infty$ of particles with masses $\{m_k\}_{k=1}^\infty$ proportional to the minimum mass of a monomer m_0 : $m_k = km_0$. In this case, the coagulation equation takes the form (see, e.g., the review (Chandrasekhar 1943, Chapter III, Section 6)):

$$\dot{N}_k = \frac{1}{2} \sum_{i+j=k} N_i N_j K_{ij} - N_k \sum_{j=1}^\infty N_j K_{kj}. \quad (2)$$

Note that only terms in which $m_i + m_j = m_k$ are included in the first (double) sum, which is equivalent to the condition $i + j = k$ for the adopted mass grid. Finding an exact solution to this equation requires tracing a large range of particle masses, which makes the grid $m_k = km_0$ unsuitable in practice. Therefore, a logarithmic grid of masses of the coagulating particles is usually used. The problem of conservation of mass arises, since two arbitrary masses from such a grid m_i and m_j are very unlikely to correspond to a k such that $m_k = m_i + m_j$. A conservative algorithm is presented in Kovetz & Olund (1969), in which the mass $m_i + m_j$ distributed between the masses for the nearest grid points to the left and right m_l and m_r . The discrete coagulation equation can then be written in the form

$$\dot{N}_k = \frac{1}{2} \sum_{i=1}^k \sum_{j=1}^k N_i N_j C_{ijk} K_{ij} - N_k \sum_{j=1}^\infty N_j K_{kj}, \quad (3)$$

$$C_{ijk} = \begin{cases} \varepsilon, & \text{if } m_k = \max_{m_n < m_i + m_j} \{m_n\}; \\ 1 - \varepsilon, & \text{if } m_k = \min_{m_n > m_i + m_j} \{m_n\}; \\ 0, & \text{otherwise,} \end{cases} \quad (4)$$

$$\varepsilon = \frac{m_r - (m_i + m_j)}{m_r - m_l}. \quad (5)$$

Even in the conservative form (3), the coagulation equation is complicated to solve. This is related to the limited length of the mantissa of the computer representation of a real number. The coagulation of particles with masses differing by 15 orders of magnitude will be comparable to the rounding errors, even using double-precision variables in the computations. Under the conditions of protoplanetary disks, the range of dust grain masses can reach 20 orders of magnitude or more. Therefore, effective (but unwieldy) algorithms have been developed, that make it possible to include a wide range of masses without the need for a transition to high-precision arithmetical computations (Brauer, Dullemond & Henning 2008). For the goals of our study, it is important to preserve the simple form (3); therefore, we chose an extensive approach based on using libraries designed for operations with real numbers with arbitrary mantissa lengths. The rising computational expenses for this case were compensated by the application of parallel-programming methods.

2.2 Coagulation Equation Kernel with Grain Charge Dispersion

The efficiency of the coagulation process is described by the kernel $K_{ij} = K(m_i, m_j)$. The case of neutral grains has been studied fairly well recently (see, e.g., Brauer, Dullemond & Henning (2008); Birnstiel, Dullemond & Brauer (2010); Zsom et al. (2010); Blum & Wurm (2008)):

$$K_{ij} = p_{ij} \pi (a_i + a_j)^2 u_{ij}, \quad (6)$$

where p_{ij} is the sticking probability for grains with radii a_i and a_j moving with relative velocity u_{ij} . We assumed that the relative velocity of the grains arises only due to Brownian motion, which corresponds to the initial stages of dust evolution (and grain sizes up to $\sim 10^{-2}$ cm at distances of 1 AU; see, e.g., Testi et al. (2014)). Other mechanisms determining the relative velocities of the grains, such as turbulence and radial and vertical drift (Brauer, Dullemond & Henning 2008) become important at

later stages of dust evolution than those considered here. Including these in models for charged dust requires a much more complex approach and is the topic of a separate study.

The charges of grains in the central regions of a disk were calculated in detail in Okuzumi (2009); Okuzumi et al. (2011a,b), where the electrostatic interaction energy for large grains (with sizes of more than 10^{-3} cm) was found to exceed their kinetic energy associated with collisions — the electrostatic barrier against dust growth referred to above.

To analyze the influence of the grain charge on the rate of their growth in more detail, we considered a general form of the coagulation kernel taking into account Coulomb focusing (Spitzer 1941):

$$K_{ij}(Q_i, Q_j) = p_{ij} \pi (a_i + a_j)^2 \left[1 - \frac{2Q_i Q_j e_p^2}{m_{ij}(a_i + a_j) u_{ij}^2} \right] u_{ij}, \quad (7)$$

where Q_i and Q_j are the charges of the grains, $m_{ij} = m_i m_j / (m_i + m_j)$ is the reduced mass, and e_p is the elementary charge. It is obvious that the additional condition $K_{ij}(Q_i, Q_j) \geq 0$ is imposed on K_{ij} . This form of the coagulation kernel (7) is valid when the mass and size of the grains uniquely determine their charge.

However, the charge of a specific grain fluctuates with time; in other words, there is a non-zero dispersion for the charge in an ensemble of grains of a given size. Let the mean charge of grain i be \bar{Q}_i and the standard deviation of the charge about the mean be σ_i . As a rule (Tielens 2005), the distribution of grains of a given size a_i over the charge q will be close to normal

$$f(q, \bar{Q}_i, \sigma_i) = \frac{1}{\sigma_i \sqrt{2\pi}} e^{-\frac{(q - \bar{Q}_i)^2}{2\sigma_i^2}}. \quad (8)$$

It is not difficult to show that the coagulation kernel transforms to the form

$$K_{ij}^* = \int f(q, \bar{Q}_i, \sigma_i) \int f(p, \bar{Q}_j, \sigma_j) K_{ij}(q, p) dq dp. \quad (9)$$

The simple replacement of K_{ij} with K_{ij}^* brings Eq.(3) for neutral grains to the discrete coagulation equation for charged grains with a non-zero charge dispersion. The sticking probability was taken to be unity. The process of fragmentation during collisions at high velocities is also important for the evolution of dust. The fragmentation barrier against dust growth is important for large grains; i.e., it becomes significant after the electrostatic barrier has been overcome. Since our aim was to search for mechanisms capable of overcoming the electrostatic barrier, we neglected grain fragmentation.

Equation (3) written for each $k = 1, \dots, N_{\text{mass}}$ represents a system of non-linear ordinary differential equations. We solved this system using an explicit 5th-order Runge–Kutta method with an adaptive step control (Press et al. 1993). Although implicit integration methods can yield a solution over a smaller number of steps, in practice, such methods proved slower due to the additional time required to compute the Jacobian.

2.3 Computation of the Dust Charge

The photoelectric effect and the accretion of electrons and ions onto a grain are the main factors determining the charge of a dust grain under most astrophysical conditions (Weingartner & Draine 2001). Thus far, only the acquisition of charge through collisions has been considered in relation to the dust growth in protoplanetary disks. In this case, the high velocities of electrons compared

to ions lead to negatively charged grains. However, as a rule (see, e.g., (Pedersen & Gómez de Castro 2011)), a positive charge may be acquired in the atmosphere of the disk due to the efficient photoelectric effect. Therefore, there should exist a region in the disk at intermediate heights where the grain charges are close to zero. The main goal of our study was a detailed consideration of this region from the point of view of the coagulation theory of charged particles. The main equations used to compute the grain charges, based on the treatment in Tielens (2005); Draine & Sutin (1987); Weingartner & Draine (2001), are presented below.

If we consider collisions of dust grains with electrons and singly charged ions, the probability $f(Z_{\text{gr}})$ of encountering a grain with charge $Z_{\text{gr}} e_p$ can be found from the detailed balance equation

$$f(Z_{\text{gr}}) [J_{\text{pe}}(Z_{\text{gr}}) + J_{\text{ion}}(Z_{\text{gr}})] = f(Z_{\text{gr}} + 1) J_e(Z_{\text{gr}} + 1), \quad (10)$$

where J_{pe} [s^{-1}] is the photoelectron emission rate and J_e and J_{ion} [s^{-1}] are the accretion rates of electrons and ions. To find the total charge distribution function $f(Z_{\text{gr}})$, the equation above is written for each value Z_{gr} , which reduces to the system

$$f(Z_{\text{gr}}) = f_0 \prod_{z=Z_0+1}^{Z_{\text{gr}}} \frac{J_{\text{pe}}(z-1) + J_{\text{ion}}(z-1)}{J_e(z)} \quad (11)$$

for $Z_{\text{gr}} > Z_0$ and

$$f(Z_{\text{gr}}) = f_0 \prod_{z=Z_{\text{gr}}}^{Z_0-1} \frac{J_e(z+1)}{J_{\text{pe}}(z) + J_{\text{ion}}(z)} \quad (12)$$

for $Z_{\text{gr}} < Z_0$. Here, $f_0 \equiv f(Z_0)$. We especially note that, from a computational point of view, it is important to choose a value of Z_0 that is close to the maximum of $f(Z_{\text{gr}})$, which can be tentatively estimated from the approximate equality

$$J_{\text{pe}}(Z_0) + J_{\text{ion}}(Z_0) \approx J_e(Z_0). \quad (13)$$

Equations (11), (12) are closed with the obvious relation

$$\sum_{Z=-\infty}^{\infty} f(Z) = 1. \quad (14)$$

The accretion rate of particles with number density n and mass m can be written (Draine & Sutin 1987):

$$J_{\text{acc}} = n \sqrt{\frac{8kT_{\text{gas}}}{\pi m}} \pi a_{\text{gr}}^2 \tilde{J}(a_{\text{gr}}, T_{\text{gas}}, Z_{\text{gr}}). \quad (15)$$

The function \tilde{J} takes into account Coulomb focusing. Following Weingartner & Draine (2001), we took the sticking probabilities for electrons and ions to be 0.5 and 1, respectively.

The photoemission rate depends on the solid-angle-averaged radiation intensity J_{ν} [$\text{erg}/(\text{cm}^2 \text{ s Hz ster})$], the absorption cross section C_{abs} and the photo-ionization yield Y (Weingartner & Draine 2001):

$$J_{\text{pe}} = \int \frac{4\pi J_{\nu}}{h\nu} C_{\text{abs}}(\nu, a_{\text{gr}}) Y(\nu, Z_{\text{gr}}, a_{\text{gr}}) d\nu \quad (16)$$

An important assumption we made is that the grains are not the dominant charge carriers in the plasma. The depth of penetration of the photons and the mean free path of the electrons in a grain were taken to be 100 \AA and 10 \AA , respectively, and the work function of the photoelectrons to be 8 eV, which corresponds to silicate grains.

3 MODELING THE GROWTH OF CHARGED GRAINS

To show how the charge of a grain influences its growth, the coagulation equation (3) was solved locally for each point in the disk for three cases. In the first, the grains were assumed to be neutral; i.e., their coagulation is not hindered (or facilitated) by electrostatic interactions. We call this case the comparison model (Model 1). In the second (Model 2), it is assumed that the charge of a grain is determined only by collisions with electrons and ions. This approximation is valid for dense regions in the disk near the midplane, where stellar radiation cannot reach. In this case, the grains become negatively charged, and the Coulomb interaction begins to hinder coagulation. Both grain-charging mechanisms are considered in Model 3 — collisional and radiative. This general case is of the most interest.

We emphasize that the coagulation equation was solved locally and independently for each point in the disk. In other words, it was assumed that there was no advective term in the coagulation equation. This assumption is very probably not satisfied for large grains in protoplanetary disks, since they are subject to settling toward the midplane and radial drift. However, such a local approach is useful when searching for possible ways to enhance the growth of grains in some part of the disk. In this case, the distribution of the mean grain size over the disk visually reflects the distribution of coagulation rates.

3.1 Model for the Physical Structure of the Disk

Since we did not aim to compute the detailed physical structure of the disk (density, temperature, radiation field), we chose the characteristic parameters of disks around single T Tauri stars (Williams & Cieza 2011). The disk was assumed to be stationary up to an age of one to three million years (Mamajek 2009), with a surface density Σ , that has a power-law dependence on the distance to the star R : $\Sigma = \Sigma_0 (R/R_0)^{p_s}$. We assumed hydrostatic equilibrium in the vertical direction. The radial profile of the temperature was determined assuming a geometrically thin disk and blackbody re-radiation of the UV flux from the star (Armitage 2010, formula (2.28)). The disk was taken to be isothermal in the vertical direction, and the gas temperature was taken to be equal to the dust temperature. The stellar radiation was taken to be blackbody radiation with the effective temperature T_* and a UV excess with effective temperature T_*^{UV} . We chose the normalization of the UV excess such that $B_{4000\text{\AA}}(T_*) = B_{4000\text{\AA}}(T_*^{UV})$. The degree of ionization was taken to be the same throughout the disk and equal to $x_e = 10^{-4}$, which corresponds to the ionization of carbon (we discuss the influence of this assumption for the model of the dust evolution below). The coagulation equation was solved locally for each point in the disk on a $N_r \times N_z$ grid.

The influence of the assumption of stationarity and the choice of disk parameters on the results obtained is discussed in Section 4. The results of our computations for Models 1–3 with the disk parameters listed in the Table 1 are presented below.

3.2 Neutral Grains

The case of neutral grains has been considered in many studies of dust evolution in protoplanetary disks. Excluding Coulomb forces from consideration leads to faster grain growth for denser regions. Since the coagulation rate is proportional to the square of the particle number density, the mean size of the grains \bar{a} depends strongly on their location in the disk (Fig. 1). Three million years

Table 1. Main parameters of the model

Parameter	Value
R_0	1 AU
Σ_0	300 g/cm ²
p_s	-1
M_{disk}	0.02 M_\odot
T_*	4000 K
T_*^{UV}	20000 K
x_e	10^{-4}
N_{mass}	64–128
N_r	15–30
N_z	15–30

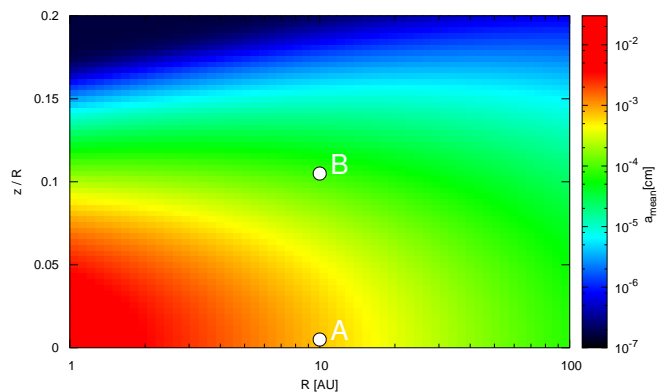


Figure 1. Distribution of the mean grain size over the disk for Model 1 at a time of three million years.

after the start of the growth, the range of the mean grain sizes in the disk reaches six orders of magnitude (18 order of magnitude in mass). Note that fragmentation can appreciably slow the dust growth rate, thereby narrowing this range. However, as was shown in Windmark et al. (2012), taking into account the velocity distribution of the grains partially solves the problem of fragmentation.

The detailed mass distributions of the grains $f(m)$ for points A and B indicated in Fig. 1 at a radius of 10 AU and various times are also presented (Fig. 2). The densities at points A and B differ by about three orders of magnitude. Figure 2 presents the quantity $m^2 f(m)$, for Model 1, which reflects the contributions of various grains to the total mass. The zero of time corresponds to a so-called MRN distribution (Mathis, Rumpl & Nordsieck 1977). The growth of the dust at points A and B occurs similarly in terms of the profiles of the distribution function $f(m)$, but on different time scales. Figures 3 and 4 show the vertical and radial profiles of the mean grain size for times $t = 1, 10^3$ and $3 \cdot 10^6$ yr. Note that the growth of neutral grains is fairly uniform in the sense that $\lg \bar{a} \sim \lg t$, which is not true for charged grains.

3.3 Collisionally Charged Grains

Under equilibrium conditions, the electrons have higher velocities than the ions, so that the grains collide more often with electrons, leading to a negative charge for the grains. As the grains grow, their negative charge also increases. Their relative velocity may also in-

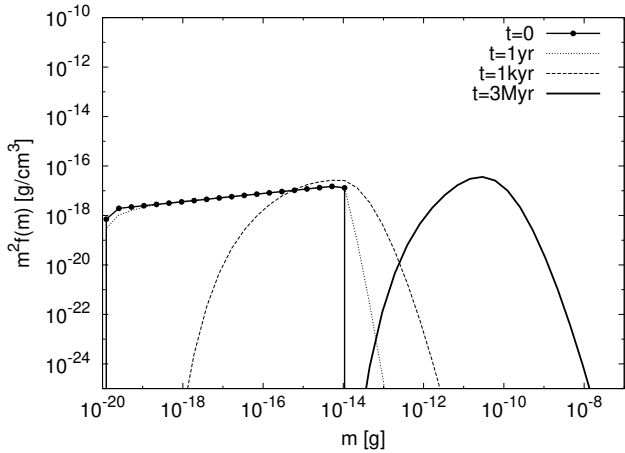
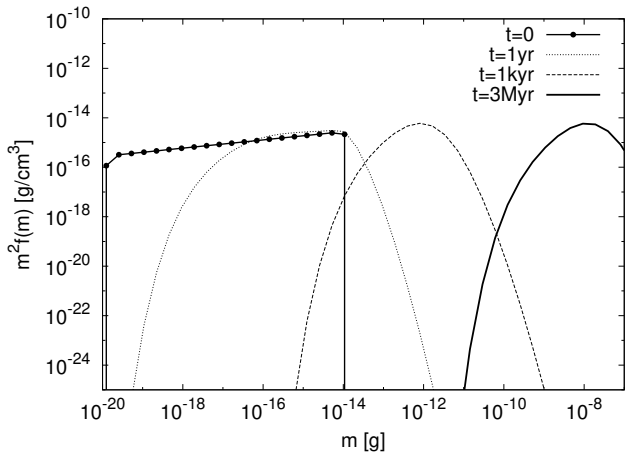


Figure 2. Mass distribution function for the grains for Model 1 (for various times) at point A (upper panel) and point B (lower panel) marked in Fig. 1.

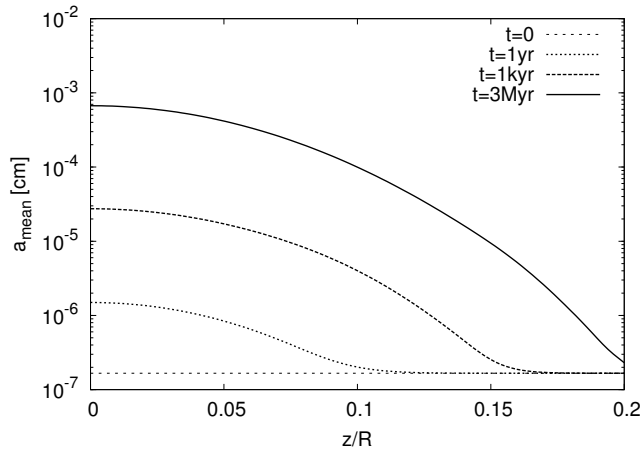


Figure 3. Vertical profile of the mean grain size at a distance of 10 AU from the star for Model 1 (for various times).

increase. Therefore, the Coulomb factor in Eq. (7) can either increase or decrease during the dust evolution. It was shown in Okuzumi (2009) that the electrostatic interaction energy begins to exceed the mean kinetic energy of grains with sizes of $\sim 10^{-3}$ cm or more, so that the growth of the grains should be appreciably suppressed. This threshold should depend on the ambient conditions, which can vary strongly over the disk. Therefore, we carried out global mod-

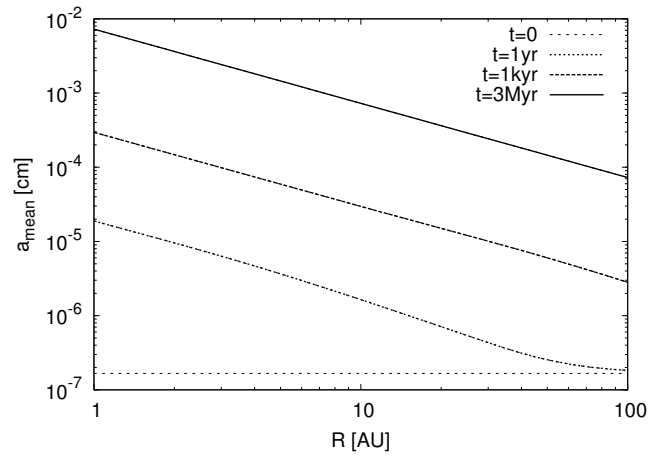


Figure 4. Radial profile of the mean grain size in the midplane of the disk for Model 1 (for various times).

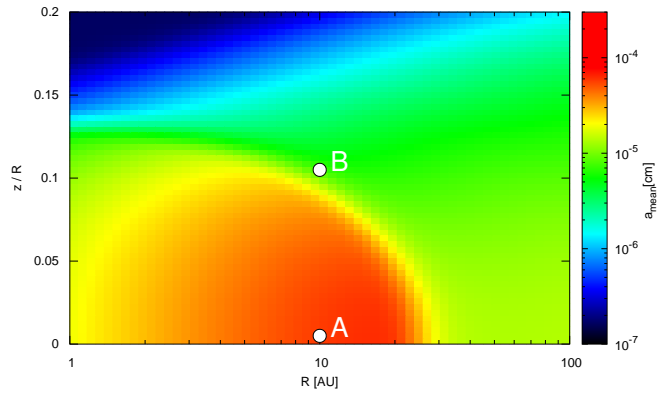


Figure 5. Same as Fig. 1 for Model 2. The upper boundary of the color scale is two orders of magnitude lower than the scale in Fig. 1.

eling of the coagulation of (negatively) charged grains in order to study the conditions for the appearance of the electrostatic barrier.

Figure 5 presents the distribution of the mean grain size over the disk, taking into account collisional charging. The growth of the dust is appreciably suppressed by its charge, and the upper boundary for the grain size shown by the color scale is two orders of magnitude lower than in Fig. 1. The main difference from the case of neutral dust is that the growth rate is not proportional to the number density. This is expressed by the fact that the grains grow most rapidly at intermediate radii $\approx 2 - 20$ AU. The grains are more strongly charged in inner, dense regions than in outer regions, making the electrostatic suppression of their growth more important there. With distance from the star, the grain charge begins to decrease in magnitude, speeding up the coagulation. The drop in density in the disk becomes important in peripheral regions, leading to slowing of the coagulation.

The mass distribution function of the charged grains also differs qualitatively from the neutral case (Fig. 6). This distribution is bimodal; this is clearly visible for point B at a time of three million years, but is also true to a lesser extent for other times and locations in the disk. The origin of this bimodality is related to the non-geometrical relationship between the interaction cross section

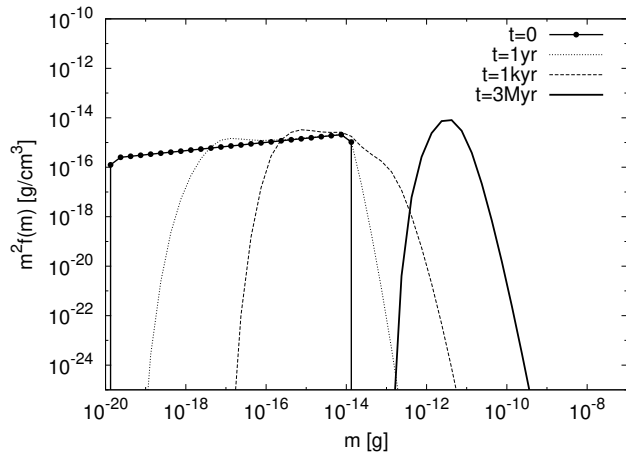


Figure 6. Same as Fig. 2 for Model 2.

and the particle size. If the mass growth rate was proportional to the geometrical cross section, particles with initially different sizes would tend to acquire more equal sizes as they grew. Additional factors, whether gravitational or electrostatic forces, change the effective collisional cross section. This means that large particles can grow more rapidly than smaller ones.

A comparison of the vertical and radial profiles of the mean grain size for Model 2 (Figs. 7 and 8) and Model 1 (Figs. 3 and 4) confirms the need to take into account the dust charge when considering its evolution. Note that the maximum of the profiles in Fig. 8 move outward during the evolution of the dust.

3.4 General Case of Charged Dust

The ejection of electrons from grains by UV photons leads to appreciably positively charged dust in the disk atmosphere. As the UV flux weakens toward the midplane, the efficiency of the photoelectric effect decreases, and the grains become less charged. At some height above the midplane, the mean grain charge becomes zero. Upper panel of Fig. 9 presents the charge vertical profile for grains of various sizes at a distance of 10 AU from the star. The mean grain charge vanishes at a height $z/R \approx 0.1$. Since the dispersion of the charge is non-zero (see lower panel of Fig. 9), grains with charges of both signs are present in this area (point B). Thus, electrostatic enhancement of the grain growth will operate in the vicinity of lines of zero charge in the disk.

Determining the charge of grains in the disk atmosphere is

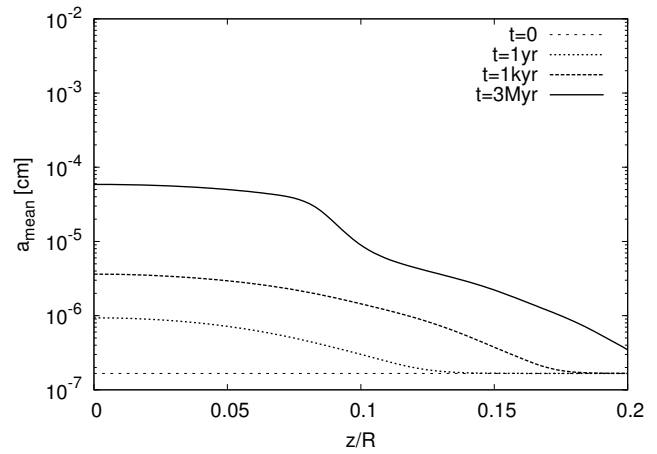


Figure 7. Same as Fig. 3 for Model 2.

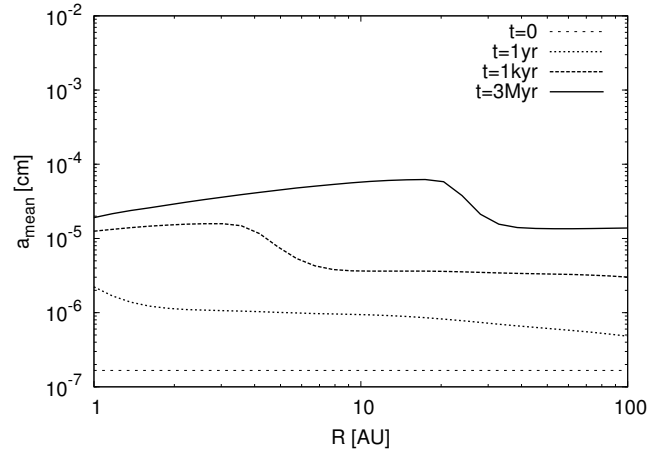


Figure 8. Same as Fig. 4 for Model 2.

directly related to the radiative transfer modeling. The deeper the UV radiation penetrates into the disk, the deeper the layer of near-zero charge lies. This facilitates the growth of grains due to their higher number density. We adopted a conservative estimate for the radiation field, and considered only radiation from the central star, taking into account extinction by grains with standard interstellar parameters (in accordance with formula (5.96) of Tielens (2005)). A number of factors (grain growth, scattering, background radiation) can lead to better penetration of radiation into the disk. Therefore, the mean grain sizes in the disk atmosphere presented below are lower limits, and the dust coagulation rates in the disk atmosphere will become higher in a more detailed consideration of the radiative transfer.

The difference in the densities at points A and B is approximately three orders of magnitude; i.e., the coagulation rates for the neutral case differ by six orders of magnitude. It turns out that this difference in coagulation rates is fully compensated due to the absence of Coulomb repulsion and switching to Coulomb focusing, and leads to an appreciable dust growth at intermediate heights (Fig. 10). The mass distribution of the grains at point B (Fig. 11) is not bimodal, and resembles the distribution for neutral dust. The dispersion of the charge in early stages (~ 1 kyr) leads to an increase in the dust growth, even compared to the neutral case. The

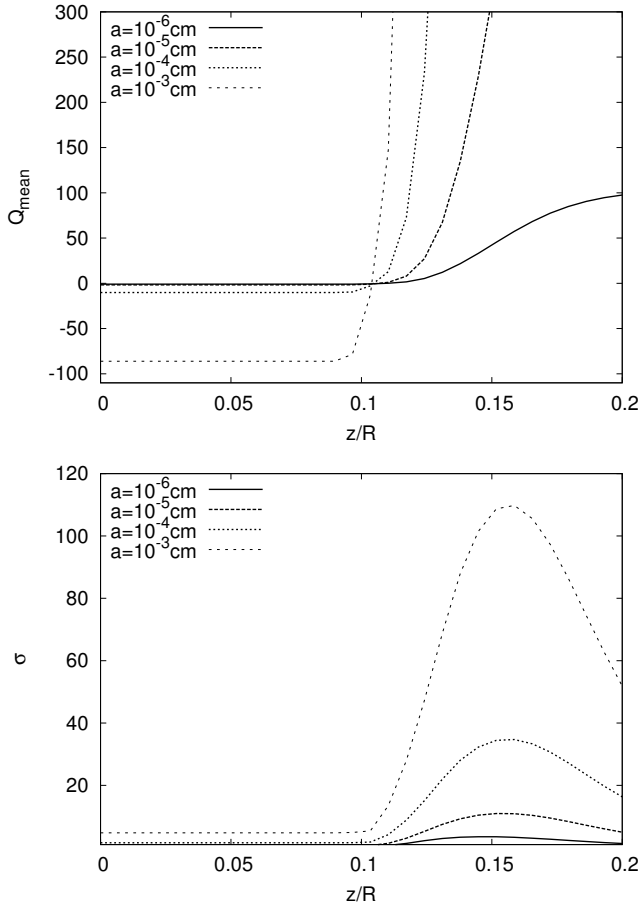


Figure 9. Vertical profiles of the mean charge (upper panel) and the standard deviation of the charge (lower panel) at a distance of 10 AU from the star (for various grain sizes a).

grains in the layer with near-zero charge are even somewhat larger than those in the dense midplane regions (Fig. 12).

This increase in the coagulation rate at the zero-charge line is a fully expected result. However, in our formulation, the mean charges of grains of all sizes vanish at the same zero-charge line, and not at various regions of space. This makes the appreciable thickness of the layer of active dust growth that comes about due to the dispersion of the dust charge an intriguing result. An additional contribution to the dispersion could also be made by differences in the work function for the emission of electrons from grains of inhomogeneous chemical composition. The absence of an electrostatic barrier at intermediate heights could play a determining role for the overall growth of dust for a disk that is undergoing sufficiently strong mixing. A simultaneous description of mixing processes and the dust growth requires substantially more complex modeling, and is an interesting topic for a separate study.

4 DISCUSSION

4.1 Influence of Dynamical Effects

The results presented in the previous section were obtained under the assumptions that the disk structure is stationary over scales of several million years, and that there is no drift of the dust relative to the gas. Turbulence, meridional circulation (Urpin 1984), and

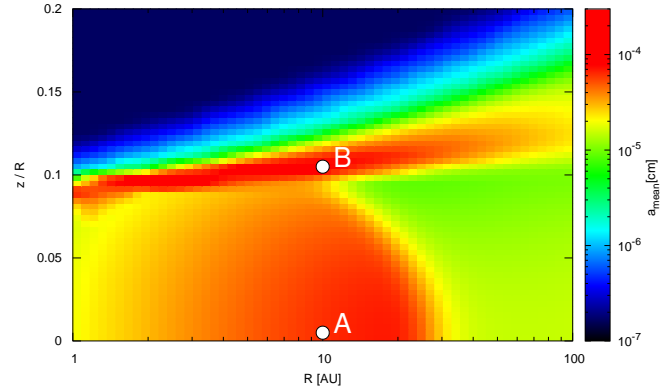


Figure 10. Same as Fig. 1 for Model 3. The upper boundary of the color scale is two orders of magnitude lower than in Fig. 1.

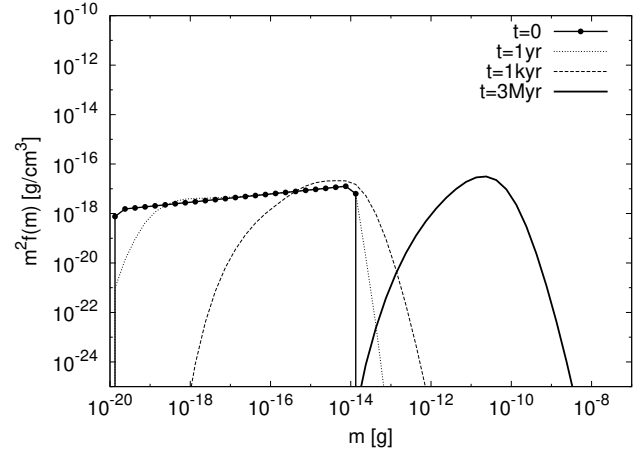


Figure 11. Mass distribution function for the grains at point B for Model 3 (for various times).

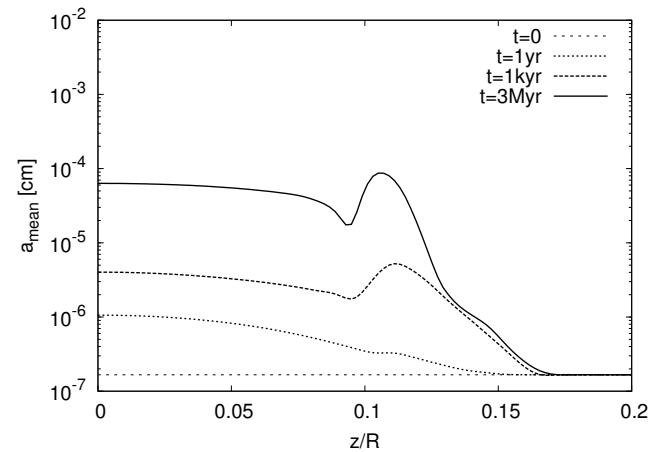


Figure 12. Same as Fig. 3 for Model 3.

sedimentation of the grains will lead to flows into and out of the layer of active dust growth. The question is whether these factors facilitate or hinder dust growth. The answer to this question could be given by appropriate modeling, but the qualitative picture can also be described based on general reasoning.

On the one hand, the flow of gas through the growth layer reduces the residence time for a specific grain in the layer. This should reduce the coagulation rate, although the same material may pass through the growth zone multiple times in the presence of global vortices or circulation in the disk. On the other hand, since small grains are efficiently dynamically coupled to the gas, the flow of gas delivers small grains to the near-zero charge layer. Due to the lower charge inside this layer, the coupling between the dust and gas falls, and the grains are decelerated. They begin to grow efficiently in this layer, which further reduces the friction between the gas and the dust per unit dust mass. Thus, the residence time of the dust in the layer grows. In other words, a stationary flow through the growth layer can lead to an increase in the dust density inside the layer, which enhances the coagulation rate.

As the grains grow, settling toward the midplane under the action of the vertical component of the gravitational force becomes important. The scale height, determined by the balance between gravitation and turbulent mixing, is smaller for larger grains. Other things being equal, the scale height for charged dust is larger than the scale height for neutral dust, due to the more effective coupling of charged grains with the gas. Thus, the charge of a grain increases the sedimentation scale height, which also enhances coagulation in the disk atmosphere.

The median lifetime of a protoplanetary disk is three million years (Williams & Cieza 2011). Disks around massive stars dissipate more rapidly than disks around solar-type stars. Therefore, the lifetimes for individual disks vary from one to ten million years. At late stages of the evolution, the dispersal of the disk occurs from inside out, shifting the inner edge of the disk beyond 1 AU from the star. In Models 1–3, the inner edge of the disk lies approximately at 0.5 AU, which corresponds to the dust sublimation radius. The stellar radiation is efficiently absorbed due to the high densities near the midplane, and does not reach distances of 1 AU, so that grains at height $z = 0$ are negatively charged. The dispersal of the disk means that radiation begins to penetrate into the disk midplane, which changes the sign of the dust charge. In this way, the layer of active dust growth (in the region of near-zero charge) moves outward along the equatorial plane, with its relatively high number density of dust grains. Since an increase in grain size leads to a decrease in opacity, this process will proceed in an accelerating regime. Therefore, the growth of dust in the region of near-zero charge can become even more important at the stage of the dispersal of the disk.

4.2 Influence of Porosity and Fluctuations of the Grain Velocities

The results presented here were obtained for compact, spherical dust grains. However, to all appearances, grains in protoplanetary disks have a very porous, fractal structure. This porosity increases the effective cross section of the grains, together with the sticking probability. Therefore, the presented mean grain sizes are lower limits for the more general case of non-compact agglomerates. Note that it was shown in Okuzumi (2009) that the charge of grains increases with their porosity.

The use of the mean relative velocity for grains of two specified masses can distort the real pattern of the dust evolution. For

example, considering the velocity distribution of grains of a single size makes it possible to lower the fragmentation barrier against dust growth (Windmark et al. 2012). As the grain size increases, the relative velocity increases, and may exceed the velocity at which fragmentation occurs. However, grains with lower velocities will always be found in the ensemble, whose collisions do not lead to fragmentation. Consideration of the dust charge provides an additional possibility for suppressing fragmentation. Since the grains in the midplane have the same charge sign, Coulomb repulsion slows particles approaching each other, lowering the fragmentation rate.

4.3 Influence of the UV Excess and Degree of Ionization

The magnitude of the UV excess determines how deep the radiation penetrates into the disk, i.e., the position of the zero-charge line. The more intense the UV excess, the faster the dust coagulation rates, since the growth layer moves deeper into the disk.

We took the degree of ionization to be constant in the disk, and equal to $x_e = 10^{-4}$, corresponding to ionized carbon. The range of physical conditions in a protoplanetary disk is very broad, and the degree of ionization varies widely, from $\sim 10^{-10}$ to unity (Semenov, Wiebe & Henning 2004). However, we used the degree of ionization only to compute the grain charges. The dust charge in the disk atmosphere is determined by the photoelectric effect, and is practically independent of x_e . The situation is the opposite in the midplane, where collisions with electrons and ions determine the dust charge. However, under the conditions of electrical neutrality, the dependence on the number density disappears, and the grain charge depends only on the ratio of the masses of the dominant ion and the electron (Tielens 2005, formula (5.70)). Thus, the degree of ionization is important only in the transition layer, where carbon is ionized and $x_e \sim 10^{-4}$. Note that the degree of ionization in deep layers of the disk could be so low that grains accrete all available electrons. Their charges will be smaller in magnitude in this case. The conclusion that the coagulation rate of the dust grains is substantially suppressed in the midplane of the disk is preserved in a self-consistent computation of the grain charge and degree of ionization (Okuzumi et al. 2011b).

5 CONCLUSION

We have considered one problem in the modern theory of planet formation — the electrostatic barrier against the early growth of dust in protoplanetary disks. Studies of the coagulation of charged particles have often assumed that dust grains acquire charge only via collisions with ions and electrons. Here, we have conducted modeling of grain growth taking into account radiative and collisional mechanisms for the acquisition of charge.

Consideration of the photoelectric effect leads to the appearance of a line of zero charge at intermediate heights in the disk (where $A_V \sim 1$). The non-zero dispersion of the grain charge gives rise to a fairly thick layer in which grains with both signs of charge are present. This removes the electrostatic barrier in a certain layer of active dust growth at intermediate heights, and opens the possibility of removing this barrier completely for a disk with efficient mixing. Global flows in the disk, vortices, meridional circulation, and turbulence should facilitate an inflow of grains into the growth region from other parts of the disk. In this case, evolved dust that has passed through the growth region will return to other areas with significant electrostatic barriers. The circumstance that the scale

height for the sedimentation of charged grains is larger than the corresponding scale height for neutral grains, due to the higher friction with gas, is important here.

If mixing mechanisms in the disk are not sufficiently strong, the proposed mechanism for removing the electrostatic barrier will not operate efficiently in the stationary stage of evolution of the disk. However, the zero-charge line will pass through the disk mid-plane, where the number density of dust and the dust coagulation rate are high, in the stage of the dispersal of the disk. In this regime, the evolution of the dust can proceed in an accelerating fashion on short time scales, due to the positive feedback between dust growth and irradiation in the disk.

ACKNOWLEDGMENTS

We thank Ya.N. Pavlyuchenkov, N.N. Chugai, and the anonymous referee for useful comments.

This work was supported by the Russian Foundation for Basic Research (nos. 13-02-00138, 14-02-31400), the Dynasty Foundation, and St. Petersburg State University (grant no. 6.38.669.2013).

REFERENCES

- Akimkin V., Zhukovska S., Wiebe D., Semenov D., Pavlyuchenkov Y., Vasyunin A., Birnstiel T., Henning T., 2013, *ApJ*, 766, 8
- Armitage P. J., 2010, *Astrophysics of Planet Formation*
- Birnstiel T., Dullemond C. P., Brauer F., 2010, *A&A*, 513, A79
- Blum J., Wurm G., 2008, *ARA&A*, 46, 21
- Brauer F., Dullemond C. P., Henning T., 2008, *A&A*, 480, 859
- Chandrasekhar S., 1943, *Reviews of Modern Physics*, 15, 1
- Draine B. T., Sutin B., 1987, *ApJ*, 320, 803
- Dullemond C. P., Dominik C., 2005, *A&A*, 434, 971
- Fortov V. E., Khrapak A. G., Khrapak S. A., Molotkov V. I., Petrov O. F., 2004, *Physics Uspekhi*, 47, 447
- Konopka U. et al., 2005, *New Journal of Physics*, 7, 227
- Kovetz A., Olund B., 1969, *Journal of Atmospheric Sciences*, 26, 1060
- Mamajek E. E., 2009, in *American Institute of Physics Conference Series*, Vol. 1158, American Institute of Physics Conference Series, Usuda T., Tamura M., Ishii M., eds., pp. 3–10
- Mathis J. S., Rumpl W., Nordsieck K. H., 1977, *ApJ*, 217, 425
- Matthews L. S., Land V., Hyde T. W., 2012, *ApJ*, 744, 8
- Nomura H., Nakagawa Y., 2006, *ApJ*, 640, 1099
- Okuzumi S., 2009, *ApJ*, 698, 1122
- Okuzumi S., Tanaka H., Takeuchi T., Sakagami M.-a., 2011a, *ApJ*, 731, 95
- Okuzumi S., Tanaka H., Takeuchi T., Sakagami M.-a., 2011b, *ApJ*, 731, 96
- Pedersen A., Gómez de Castro A. I., 2011, *ApJ*, 740, 77
- Press W. H., Teukolsky S. A., Vetterling W. T., Flannery B. P., 1993, *Numerical Recipes in FORTRAN; The Art of Scientific Computing*, 2nd edn. Cambridge University Press, New York, NY, USA
- Safronov V. S., 1969, *Evoliutsiia doplanetnogo oblaka*.
- Schmitt W., Henning T., Mucha R., 1997, *A&A*, 325, 569
- Semenov D., Wiebe D., Henning T., 2004, *A&A*, 417, 93
- Smoluchowski M. V., 1916, *Zeitschrift für Physik*, 17, 557
- Spitzer, Jr. L., 1941, *ApJ*, 93, 369
- Tanaka H., Himeno Y., Ida S., 2005, *ApJ*, 625, 414
- Teiser J., Wurm G., 2009, *MNRAS*, 393, 1584
- Testi L. et al., 2014, *ArXiv e-prints*
- Tielens A. G. G. M., 2005, *The Physics and Chemistry of the Interstellar Medium*
- Urpin V. A., 1984, *Sov.Ast.*, 28, 50
- Voelk H. J., Jones F. C., Morfill G. E., Roeser S., 1980, *A&A*, 85, 316
- Wada K., Tanaka H., Suyama T., Kimura H., Yamamoto T., 2009, *ApJ*, 702, 1490
- Weidenschilling S. J., 1977, *MNRAS*, 180, 57
- Weingartner J. C., Draine B. T., 2001, *ApJS*, 134, 263
- Williams J. P., Cieza L. A., 2011, *ARA&A*, 49, 67
- Windmark F., Birnstiel T., Ormel C. W., Dullemond C. P., 2012, *A&A*, 544, L16
- Zsom A., Ormel C. W., Güttler C., Blum J., Dullemond C. P., 2010, *A&A*, 513, A57